scientific reports

Check for updates

OPEN

Biofilm proficient *Bacillus subtilis* prevents neurodegeneration in *Caenorhabditis elegans* Parkinson's disease models via PMK-1/p38 MAPK and SKN-1/Nrf2 signaling

Marcos Francisco & Roberto Grau✉

Parkinson's disease (PD) is a no-curable neurodegenerative disease of pandemic distribution for which only palliative treatments are available. A hallmark of PD is injury to dopaminergic neurons in the substantia nigra pars compacta. Here, we report that *Caenorhabditis elegans* colonized by biofilm-forming *Bacillus subtilis* is resistant to injury of dopaminergic neurons caused by treatment with the PD-related neurotoxin 6-hydroxydopamine (6-OHDA). Biofilm-forming *B. subtilis*-colonized *C. elegans* display dopamine-dependent behaviors indistinguishable from those of 6-OHDA-untreated worms colonized by gut commensal *E. coli* OP50. In *C. elegans* PD model strains with early dopaminergic neuron decay or overexpressing human alpha-synuclein, biofilm-forming *B. subtilis* colonization had neuroprotective effects and prevents alpha-synulcein aggregation, respectively. The *B. subtilis*-controlled insulin/IGF-1 signaling (ILS), whose downregulation prevents aging-related PD, is not involved in protecting against 6-OHDA-related injury. We demonstrate that biofilm-forming *B. subtilis* activates PMK-1 (p38 MAPK)/SKN-1 (Nrf2) signaling, which protects *C. elegans* from 6-OHDA-induced dopaminergic neuron injury.

Keywords *Caenorhabditis elegans*, *Bacillus subtilis*, Probiotics, Nrf2 signaling, Parkinson disease

Parkinson disease (PD) is the second most common neurodegenerative disorder affecting the human brain[1,2]. A hallmark of PD is the loss of dopaminergic neurons within the substantia nigra in the central nervous system (CNS), which participate in important biological processes such as movement, motivation and intellectual function[3]. As PD progresses, even simple movements become difficult, and patients commonly develop dementia[1–3]. Both genetic and environmental factors influence the development and progression of PD[1–3]. The α-Synuclein (α-Syn)-encoding gene *SNCA* was the first gene found to be associated with PD[4]. α-Syn is localized at nerve terminals and plays an important but poorly understood role in neurotransmission and membrane remodeling[5,6]. In PD, α-Syn is misfolded and aggregates as toxic β-sheets, which first cause of the nonmotor and motor symptoms of the disease[7]. Other genetic markers that increase the risk of PD include the *PARK-7*[8], *PARK-2*[9], *PINK1*[10], and *LRRK*[11] genes (which encode a peroxiredoxin that stabilizes Nfr2, an E3 ubiquitin ligase or human Parkin, a PTEN-induced kinase, and a leucine-rich repeat kinase, respectively). Loss-of-function or toxic-gain-of-function mutations in these genes result in the development of autosomal (recessive or dominant) forms of genetic PD[3,12]. Among the environmental factors that increase the risk of sporadic PD are exposure to chemical products that cause oxidative damage to dopaminergic neurons, such as insecticides (i.e., rotenone), herbicides (i.e., paraquat) and toxins (i.e., 6-hydroxydopamine, 6-OHDA), which selectively inhibit the mitochondrial electron transport chain in dopaminergic neurons[1–3,13].

PD is accompanied by chronic gastrointestinal (GI) disorders (i.e., constipation, inflammation, microbiota alterations, and gut barrier compromise) that can precede motor symptoms and the diagnosis of PD by years or decades[14,15]. One still debated hypothesis regarding the etiology of PD is that, in some patients, the disease might start at the level of the enteric nervous system (ENS) in the GI tract. In this so-called "second brain"[16], α-Syn is misfolded and aggregates upon exposure of the gut to oxidative and inflammatory agents such as toxins

Departamento de Microbiología, Facultad de Ciencias Bioquímicas y Farmacéuticas, Universidad Nacional de Rosario, CONICET-Argentina, Kyojin Laboratories S.A. Castellanos 1335, 2000 Rosario, Santa Fe, Argentina. ✉email: robertograu@fulbrightmail.org

and microbial pathogens[17,18]. Misfolded α-Syn spreads through the vagus nerve to the CNS, where it induces prion-like aggregation of normal α-Syn in the brain to form pathological aggregates that might trigger the development of PD[16–18]. In addition to gut comrpomise[15] and genetic[12] and environmental risk factors[13], aging represents the main causative factor for PD[19,20]. This is likely because aging hinders the response of body to the detrimental effects of multiple PD risk factors[19,20]. Interestingly, interference with insulin/IGF-1 signaling (ILS) was shown to be neuroprotective in *C. elegans* models of age-related PD (e.g., *daf-2* mutants)[21]. However, the clinical translation of methods involving the genetic manipulation of *daf-2* (IGF1 receptor) to humans (i.e., CRISPR- or RNAi-mediated gene inactivation) is limited because of the detrimental side effects that can arise from genetic interference with insulin or IGF1 signaling (i.e., diabetes development, cancer, growth deficiency and dwarfism)[12,22]. Based on the hypothesis that the probiotic bacterium *Bacillus subtilis*[23–25] delays aging in *C. elegans* by decreasing the activity of ILS[26], we and others demonstrated that different probiotic strains of *B. subtilis* were able to prevent the toxic aggregation of α-Syn and extend the lifespan of *C. elegans* overexpressing α-Syn in muscle cells[27,28].

According to epidemiological studies, there are more than five million individuals with PD[1,2]. It is believed that the number of PD cases will double over the current decade, suggesting that PD is a new pandemic[2]; moreover, significant efforts have been made to identify pharmacologic treatments for preventing, delaying the progression of or curing the disease. Unfortunately, all the strategies for treating PD that have been studied thus far have failed; PD has no cure, and only symptomatic treatments are available[1,3,18]. Here, we found that biofilm-forming *B. subtilis* prevents 6-OHDA-induced neurodopaminergic injury in *C. elegans* by activating the PD-related master regulator of stress response PMK-1/SKN-1 (p38MAPK/Nrf2 in mammals).

Results

Biofilm-forming *B. subtilis* prevents the aggregation of human alpha-synuclein in PD model *C. elegans*

In 2018, we reported the ability of the probiotic *B. subtilis* strain DG101[25,29–32] to prevent the aggregation of human α-synuclein (tagged to GFP) in the muscle cells of transgenic *C. elegans*[27]. Later, in 2020, the Doitsidou M. laboratory obtained similar results using a different probiotic *B. subtilis* strain (i.e., the PXN1 strain)[28]. One attribute present in probiotic *B. subtilis* strains is their ability to make robust and sophisticated biofilms[25]. However, the proficiency in biofilm formation is not exclusive of probiotic *B. subtilis* because non-probiotic *B. subtilis* strains (for example, the laboratory model strain NCIB3610 used in this work) also form robust biofilms[26]. *B. subtilis* NCIB3610 prevented the aggregation of GFP-tagged human α-synuclein in transgenic *C. elegans* (Fig. 1a,b). There were ~ 77% fewer GFP-tagged human α-synuclein aggregates and the aggregates were ~ 34% smaller in worms colonized by *B. subtilis* NCIB3610 than in worms colonized by the commensal *E. coli* OP50 (Fig. 1e,f, Supplementary Tables 1–2). We wondered if the *B. subtilis* proficiency in biofilm formation was required to protect against the aggregation of human α-synuclein in transgenic *C. elegans*. As a model of biofilm-deficient *B. subtilis* we selected a NCIB3610-derived isogenic mutant deficient in BslA synthesis (Δ*bslA*)[26,33]. BslA is a hydrophobin that covers the *B. subtilis* biofilm, and is indispensable for biofilm formation and efficient gut colonization (Fig. S1). The biofilm formation proficiency of *B. subtilis* NCIB3610 was crucial for the complete protection against the aggregation of GFP-tagged human α-synuclein in transgenic worms (Fig. 1c). Compared with the α-synuclein aggregation in worms colonized by *E. coli* OP50, the number and size of GFP-tagged human α-synuclein aggregates in worms colonized by biofilm-deficient (Δ*bslA*) *B. subtilis* moderately decreased (Fig. 1e,f, Supplementary Tables 1–2). However, the average number and size of GFP-tagged human α-synuclein aggregates significantly increased in worms colonized by Δ*bslA B. subtilis* compared with worms colonized by biofilm-proficient *B. subtilis* (Fig. 1e,f, Supplementary Tables 1–2).

B. subtilis requires the proficiency in cell to cell communication (i.e., quorum sensing, QS) in order to build up a mature biofilm[26,34]. Similarly, to the proficiency in biofilm formation, the proficiency in QS was required to avoid the formation of human α-synuclein aggregates in *B. subtilis*-colonized *C. elegans* (Fig. 1d). Compared with colonization by wild-type *B. subtilis*, colonization with a QS-deficient (Δ*csf*)[26,33] *B. subtilis* resulted in an increase in the average number and size of GFP-tagged human α-synuclein aggregates in worms (Fig. 1e,f, Supplementary Tables 1–2). The results indicate the requirement of active QS (i.e., CSF production) and biofilm formation, for the ability of *B. subtilis* to decrease GFP-tagged human α-synuclein production in transgenic worms. As expected, the simultaneous colonization of worms by a mixture of Δ*bslA* and Δ*csf B. subtilis* cells restored the average number and size of GFP-tagged human α-synuclein aggregates to the (low) levels observed in worms colonized by wild-type *B. subtilis* (Fig. 1e,f, Supplementary Tables 1–2).

Biofilm-forming *B. subtilis* protects *C. elegans* from 6-OHDA-induced neuronal dopaminergic damage

The decreased aggregation of the PD-related neuronal protein (α-synuclein) in the muscle cells of transgenic *C. elegans* (Fig. 1) opens the possibility that biofilm-proficient *B. subtilis* could protect PD-related neurons (i.e., dopaminergic neurons). The neurotoxin 6-OHDA (an oxidation product of dopamine)[35] dose-dependently causes dopaminergic neurodegeneration and death in *C. elegans* and other PD model organisms (Fig. S2, Supplementary Table 3). To obtain insights into the ability of *B. subtilis*, and the role of its biofilm, to protect against dopaminergic neurodegeneration, we exposed *B. subtilis*-colonized wild-type Bristol N2 worms[26] to the neurotoxin 6-OHDA. Five days after treatment with 6-OHDA, the dopamine-dependent behaviors of *C. elegans* (i.e., the basal slowing response to food) were analyzed[21]. As shown in Fig. 2a, treatment with 6-OHDA caused a significant decrease of the basal slowing response in 5-day old *E. coli* OP50-fed N2 nematodes. In contrast, feeding nematodes *B. subtilis* exerted a protective effect (Fig. 2a, Supplementary Table 4). Interestingly, *B. subtilis* improved the basal slowing response in 5-day old untreated nematodes (Fig. 2a, Supplementary Table 4). A similar protective effect against changes in the ethanol avoidance response, which is a dopamine-dependent

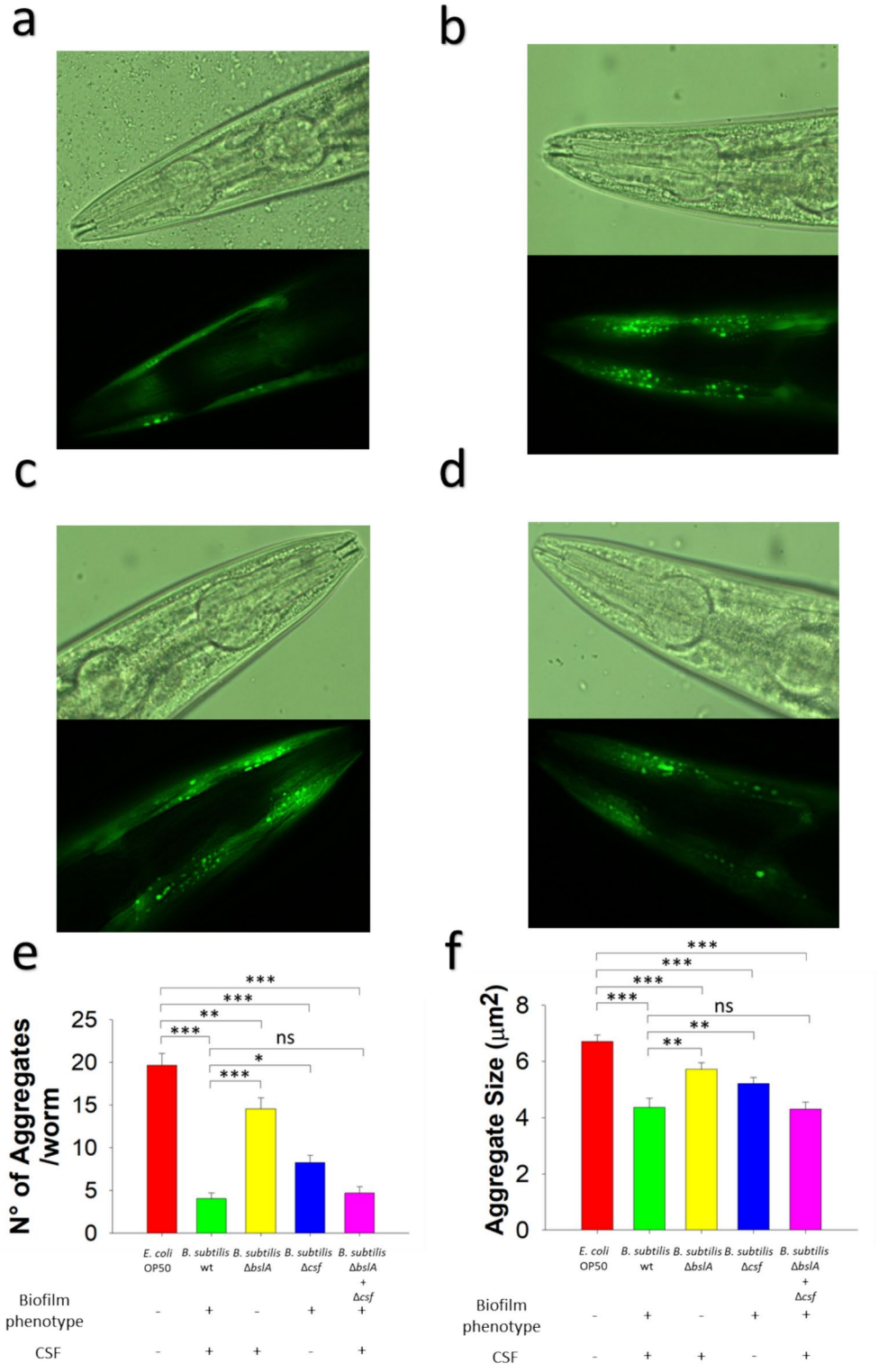

Fig. 1. Biofilm-proficient *B. subtilis* prevents human α-synuclein aggregation in a *C. elegans* model of PD. Fluorescence images of the aggregation of human α-synuclein in 7-day-old NL5901 worms colonized with biofilm-forming *B. subtilis* (**a**), *E. coli* OP50 (**b**), biofilm-deficient (Δ*bslA*) *B. subtilis* (**c**), or quorum sensing-deficient (Δ*csf*) *B. subtilis* (**d**). (e–f) The number of human α-synuclein aggregates per worm (**e**) and average size of human α-synuclein aggregates (**f**) following colonization by the indicated bacteria. Each graph (**e**,**f**) shows the average ± s.e.m. (n = 3); ns, not significant; $p > 0.05$, $^{*}p < 0.05$, $^{**}p < 0.01$, $^{***}p < 0.001$ (ANOVA followed by Bonferroni's test).

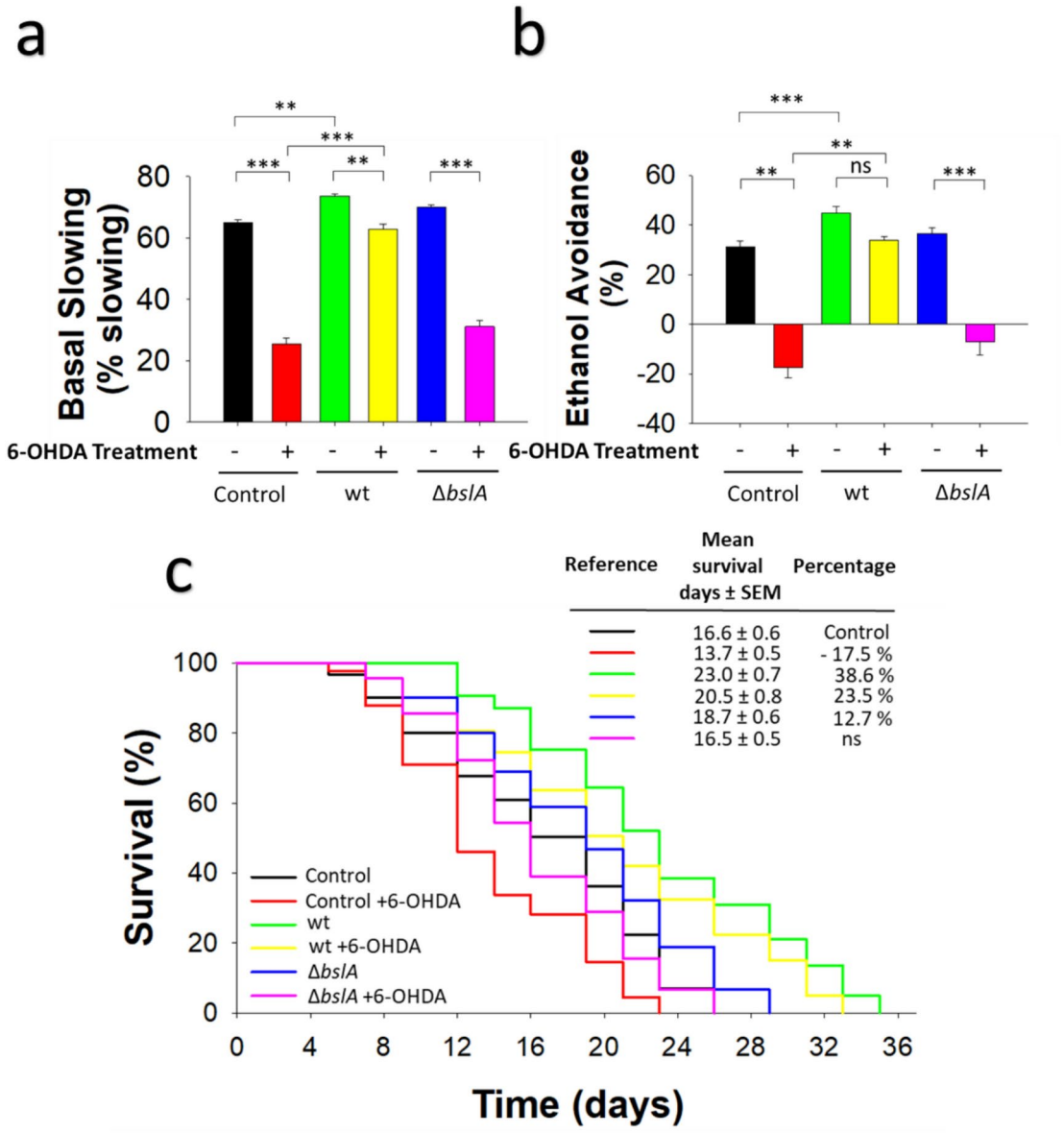

Fig. 2. Biofilm-proficient *B. subtilis* protects against the neurotoxic effects of 6-hydroxydopamine (6-OHDA) in *C. elegans*. (**a**,**b**) The basal slowing (**a**) and ethanol avoidance (**b**) responses of 5-day-old *E. coli* OP50-, biofilm-forming *B. subtilis*-, and Δ*bslA B. subtilis*-colonized N2 worms treated with (+) or without (−) 6-OHDA. (**c**) Survival of N2 worms colonized with *E. coli* OP50, biofilm-forming *B. subtilis* or Δ*bslA B. subtilis* and treated with or without 6-OHDA. Each graph (**a**–**c**) shows the average ± s.e.m. (n = 3); ***$p < 0.001$; **$p < 0.01$; *ns* no significant difference, $p > 0.05$ (ANOVA followed by Bonferroni's test). The 6-OHDA was used at a concentration of 75 mM, see Methods for experimental details.

behavior, following 6-OHDA treatment was observed in N2 worms fed *B. subtilis* compared with N2 worms fed *E. coli* OP50 (Fig. 2b). Five-day-old adult N2 worms fed *E. coli* OP50 and treated with 6-OHDA showed a dramatic decrease in the ethanol avoidance response relative to that of N2 worms not treated with 6-OHDA and fed *E. coli* OP50 (Fig. 2b). In contrast, the ethanol avoidance response of *B. subtilis*-fed N2 worms treated with the neurotoxin did not significantly differ from that of *B. subtilis*-fed N2 worms not treated with the neurotoxin (Fig. 2b, Supplementary Table 5).

Coincident with the neurotoxic effects of the drug, the lifespan of *E. coli* OP50-colonized N2 worms treated with 6-OHDA decreased relative to that of *E. coli* OP50-colonized N2 worms not treated with 6-OHDA (Fig. 2c). Compared with that of 6-OHDA-treated *E. coli* OP50-colonized N2 worms, the lifespan of 6-OHDA-treated N2 *C. elegans* colonized by *B. subtilis* was significantly extended (Fig. 2c, Supplementary Table 6).

The basal slowing- and ethanol avoidance-response were similarly affected in Δ*bslA B. subtilis*-colonized N2 worms as in *E. coli* OP50-colonized N2 worms following treatment with the neurotoxin (Fig. 2a,b, Supplementary Tables 4–5). These results are in accordance with the observed decrease in life expectancy in Δ*bslA B. subtilis*-

colonized N2 worms treated with 6-OHDA compared with biofilm-forming *B. subtilis*-colonized N2 worms treated with the neurotoxin (Fig. 2c, Supplementary Table 6).

Biofilm-forming *B. subtilis* protects *C. elegans* from aging-related dopaminergic neurodegeneration

To further elucidate the mechanism by which *B. subtilis* protects against dopaminergic damage in *C. elegans*, we used BZ555 worms, which exhibit a wild-type phenotype and in which the four pairs of dopaminergic neurons (4 CEP neurons and 2 ADE neurons in the head zone and 2 PDE neurons in the tail region) are tagged with GFP and thus fluoresce (Pdat-1::GFP)[21]. This allows natural dopaminergic neurodegeneration to be monitored by fluorescence microscopy analysis as the BZ555 worms age (Fig. 3a). Semiquantitative data reflecting the disruption of neuronal (CEP and ADE) architecture in BZ555 worms fed *E. coli* OP50 or *B. subtilis* are shown in Fig. 3b,c (see "Methods" for details). There were no differences in neuronal architecture between young adult (i.e., 4-day-old) *E. coli* OP50- and *B. subtilis*-colonized BZ555 worms, as both worm populations showed 100% dopaminergic neuronal integrity (Fig. 3b,c). However, at advanced ages (i.e., 12 and 18 days of age), a significantly higher proportion of the *E. coli* OP50-colonized BZ555 worms showed more deterioration of neuronal integrity than *B. subtilis*-colonized BZ555 worms (Fig. 3b,c, Supplementary Table 7). At 20 days of age, the 100% of *E. coli* OP50-colonized BZ555 worms showed dopaminergic neurodegeneration, while ~ 30% of *B. subtilis*-colonized BZ555 worms of the same age displayed normal neuronal architecture without signs of injury (Fig. 3b,c, Supplementary Table 7). At 24 days of age, a significant proportion of the *B. subtilis*-colonized worms exhibited intact neuronal architecture that is lost at 28 days of age (Fig. 3c, Supplementary Table 7). Overall, the mean number of days for which neurons remained intact was ~ 50% greater in *B. subtilis*-colonized BZ555 worms than in *E. coli* OP50-colonized BZ555 (Fig. 3d, Supplementary Table 8), and accordingly compared with the lifespan of BZ555 worms colonized by *E. coli* OP50, the lifespan of BZ555 worms fed *B. subtilis* increased (Fig. 3e, Supplementary Table 9).

The *B. subtilis* proficiency to form a biofilm was essential to fully protect the dopaminergic neurons of BZ555 worms (Fig. 3d, Supplementary Table 8) and to extend the lifespan of these worms (Fig. 3e, Supplementary Table 9). The mean percentage of surviving dopaminergic neurons in Δ*bslA B. subtilis*-colonized BZ555 worms was similar to that in *E. coli* OP50-colonized BZ555 worms (Fig. 3d, Supplementary Table 8). Similarly, the lifespan of Δ*bslA B. subtilis*-colonized BZ555 worms was comparable to that of *E. coli* OP50-colonized BZ555 worms (Fig. 3e, Supplementary Table 9). Compared with biofilm-forming *B. subtilis*, Δ*bslA B. subtilis* was ~ 25% and ~ 20% less effective at protecting neurons and extending the lifespan in BZ555 worms, respectively (Fig. 3d,e, Supplementary Tables 8–9).

The *B. subtilis* proficiency in QS was required for complete protection of dopaminergic neurons in BZ555 worms (Fig. 3f, Supplementary Table 10). QS-deficient (Δ*csf*) *B. subtilis*-colonized BZ555 worms showed similar behavior to that of *E. coli* OP50-colonized BZ555 worms of similar age (Fig. 3f, Supplementary Table 10). Compared with colonization by wild-type *B. subtilis* NCIB3610, colonization with Δ*csf B. subtilis* reduced the average percentage of surviving dopaminergic neurons by ~ 30% (Fig. 3f, Supplementary Table 10). The synergistic neuroprotective effects of biofilm and QS were confirmed by the full restoration of dopaminergic neuron protection in BZ555 worms simultaneously colonized by Δ*blsA* and Δ*csf B. subtilis* mutant strains (biofilm-deficient/CSF-producing and biofilm-forming/CSF-deficient strains, respectively) (Fig. 3f, Supplementary Table 10).

Biofilm-forming *B. subtilis* protects *C. elegans* from early dopaminergic neurodegeneration

The tyrosine hydroxylase CAT–2, which converts L-tyrosine to L-DOPA, the direct precursor of dopamine, is a rate-limiting enzyme in dopamine biosynthesis. In UA57 worms (which dopaminergic neurons are GFP-tagged) the excess of dopamine synthesis, due to cat-2 overexpression (i.e., *dat-1p::CAT-2*), results in the degeneration of dopaminergic neurons. This neurodegeneration has been hypothesized (although it has not been proven) to be caused by the oxidative stress provoked by the putative generation of reactive oxygen species (ROS) in UA57 worms[21,35]. Interestingly, in biofilm-forming *B. subtilis*-colonized UA57 worms the exclusive dopaminergic neuronal damage (due to dopamine excess) was dramatically delayed compared with UA57 worms colonized by *E. coli* OP50 (Fig. 4a,b, Supplementary Table 11). At 14 day of age, the 100% of dopaminergic neurons in *E. coli* OP50-colonized UA57 worms were damaged, while *B. subtilis* extends the neuronal protection up to 18 days of age (Fig. 4b,c and Supplementary Tables 11–12). Accordingly, the lifespan of UA57 worms fed *B. subtilis* significantly increased compared with the lifespan of *E. coli* OP50-colonized UA57 worms (Fig. 4d, Supplementary Table 13).

The ability of *B. subtilis* to form a biofilm was crucial for the protection of dopaminergic neurons in UA57 worms (Fig. 4c, Supplementary Table 12), and for extending the life expectancy of these worms (Fig. 4d, Supplementary Table 13). Δ*bslA B. subtilis*-colonized UA57 worms showed dopaminergic neurodegeneration slightly higher and a similar lifespan than the ones observed in *E. coli* OP50-colonized UA57 worms (Fig. 4c,d, Supplementary Tables 12–13).

The *B. subtilis* proficiency in QS was required to completely protect dopaminergic neurons in UA57 worms, although to a lesser extent than its ability to form biofilm (Fig. 4e, Supplementary Table 14). The synergistic full neuroprotective effects of *B. subtilis* biofilm and QS on UA57 worms was confirmed by the full restoration of dopaminergic neuron protection in UA57 worms simultaneously colonized by equal amounts of Δ*bslA* and Δ*csf B. subtilis* cells (Fig. 4e, Supplementary Table 14).

Having shown that biofilm-forming *B. subtilis* prevents the accelerated degeneration of dopaminergic neurons in UA57 worms, we corroborate the ability of *B. subtilis* to protect or improve behaviors under dopaminergic control in UA57 worms. The basal slowing and ethanol avoidance responses (Fig. 4f,g, Supplementary Tables 15–16), which are dopamine-dependent behaviors, of *E. coli* OP50-colonized UA57 worms were dramatically

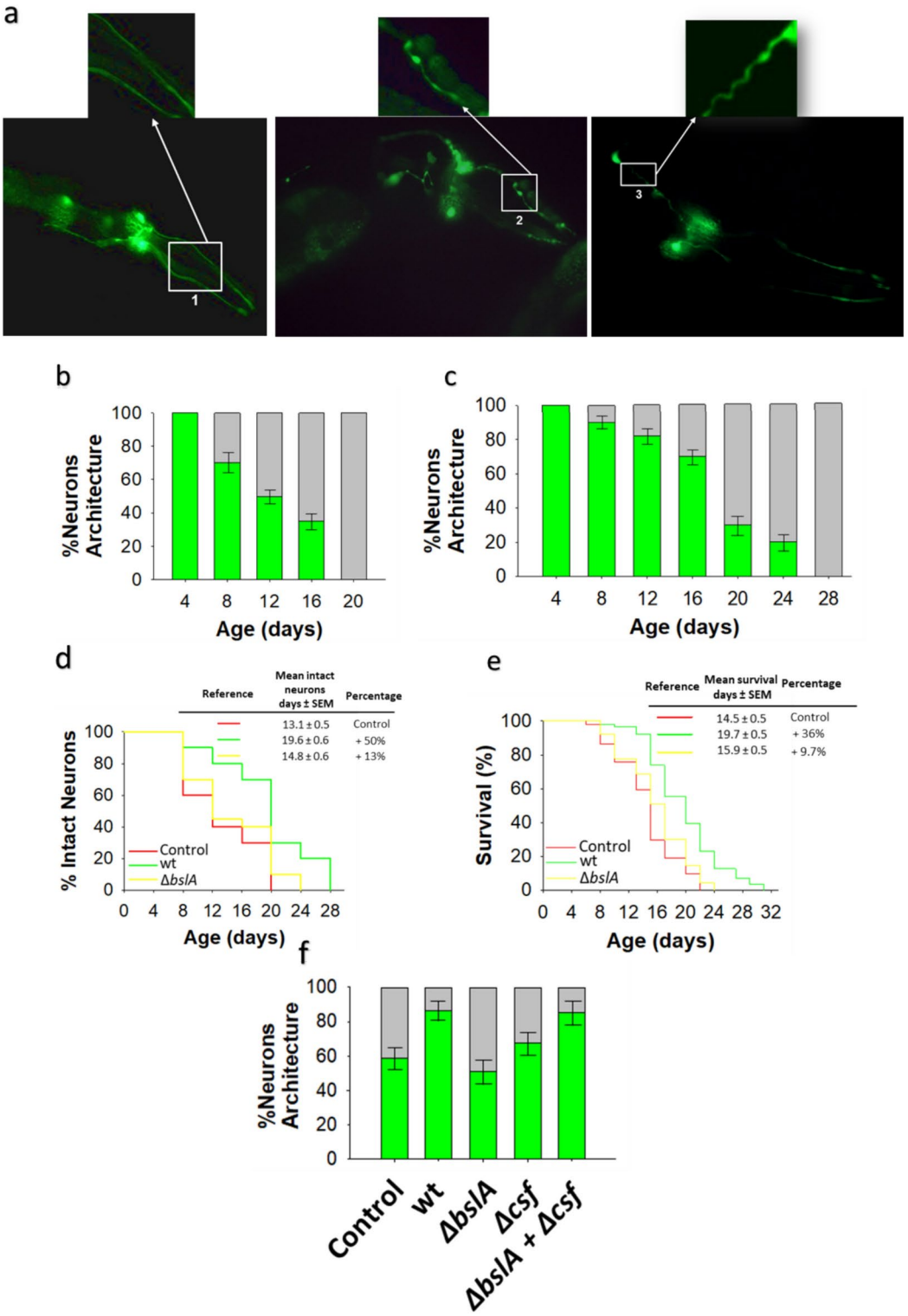

weaker than those of N2 worms colonized by *E. coli* OP50. Biofilm-forming *B. subtilis* was able to restore both dopamine-dependent behaviors in UA57 worms to a level similar to that observed in N2 worms colonized by *E. coli* OP50 (Fig. 4f,g, Supplementary Tables 15–16). In all cases, the ability of *B. subtilis* in biofilm formation and QS, and the synergistic effects of both proficiencies, for the complete recovery of dopamine-dependent behaviors was confirmed (Fig. 4f,g, Supplementary Tables 15–16).

Biofilm-forming *B. subtilis* protects *C. elegans* dopaminergic neurons from 6-OHDA-induced damage through PMK-1 and SKN-1 signaling

Aging represents the main risk factor for the development of PD[19,20]. To determine whether delayed aging underlies the protective effect exerted by *B. subtilis* against the damage to dopaminergic neurons induced by 6-OHDA (Figs. 2, 3, 4), we monitored dopaminergic-dependent behaviors (i.e., the basal slowing response) after

◀**Fig. 3**. Age-related dopaminergic neuron degeneration is delayed by biofilm-forming *B. subtilis*. (**a**) Fluorescence images of GFP-tagged dopaminergic neurons of the head region of *C. elegans* of different ages. Pictures show the neuronal architecture of dopaminergic neurons (CEP and ADE) of *E. coli* OP50-colonized BZ555 worms of 5 days (left image) and 12 days (middle and right images) of age. Normal neuronal architecture (left); damaged neuronal architecture: blebbing neurite (middle), and wavy neurite (right). (**b**,**c**) The degeneration of dopaminergic neurons in the head region of BZ555 worms colonized by *E. coli* OP50 (**b**) or biofilm-forming *B. subtilis* (**c**). Neuronal degeneration was assessed by semiquantification of the expression of GFP under the control of the *dat-1* promotor in the four CEP and two ADE dopaminergic neurons in worms of different ages using a confocal scanning microscope. The percentages of worms with normal neuronal integrity (i.e., worms with absence of dopaminergic neuronal damage, green) and worms presenting dopaminergic neuronal damage (gray) are indicated. See the Methods section for details. (**d**,**e**) The percentage of *E. coli* OP50 (red)-, biofilm-forming *B. subtilis* (green)-, Δ*bslA B. subtilis* (yellow)-colonized BZ555 worms with intact neuronal architecture over time and the lifespan of these worms are showed (**d**,**e**, respectively). (**f**) Semiquantification of dopaminergic neurodegeneration in 8-day-old BZ555 worms colonized by *E. coli* OP50, biofilm-forming *B. subtilis* or its isogenic mutants Δ*bslA*, Δ*csf*, or equal amounts of Δ*bslA* and Δ*csf* cells. Semiquantitative dopaminergic neurodegeneration data are presented as the average of three biological replicates, and the error bars represent the standard errors of the mean. Experiments were done by triplicate using 90 animals in each experiment.

treatment with 6-OHDA of worms affected in the activity of different signal transduction pathways involved in aging (i.e., the insulin-like -ILS-, and dietary restriction -DR- pathways). Compared with that of age-matched *E. coli* OP50-colonized *daf-2* worms not treated with 6-ODHA, the basal slowing response of aged *daf-2* worms fed *E. coli* OP50 and treated with 6-OHDA was severely impaired (Fig. 5a, Supplementary Table 17). This result suggest that PD-related 6-OHDA injury to dopaminergic neurons is not prevented in long-lived worms. Accordingly, the basal slowing responses of 6-OHDA treated *E. coli* OP50-colonized long-lived *clk-1* and *daf-2;clk-1* worms were severely affected compared with the responses of untreated *E. coli* OP50-colonized *clk-1* and *daf-2;clk-1* worms (Fig. 5b,c, Supplementary Table 17).

Interestingly, gut colonization by biofilm-forming *B. subtilis* in aged *daf-2*, *clk-1* and *daf-2;clk-1* worms completely protected against the toxic effects of 6-OHDA on dopaminergic neurons compared with untreated *daf-2*, *clk-1*, or *daf-2;clk-1* worms colonized by *E. coli* OP50 or biofilm-forming *B. subtilis* (Fig. 5a–c, Supplementary Table 17). Overall, protection against dopaminergic neuron injury induced by 6-OHDA was increased ~ 230%, ~ 212%, and ~ 125% in biofilm-forming *B. subtilis*-colonized *daf-2*, *clk-1* and *daf-2;clk-1* worms compared with the same worm strains colonized by *E. coli* OP50 and treated with the neurotoxin (Fig. 5a–c, Supplementary Table 17).

The ability of *B. subtilis* to protect against the dopaminergic neurotoxicity of 6-OHDA largely depended on its ability to produce biofilm. Protection against the effect of 6-ODHA was significantly decreased in Δ*bslA B. subtilis*-colonized aged *daf-2*, *clk-1* and *daf-2;clk-1* worms compared with responses of the same worm strains colonized by biofilm-proficient *B. subtilis* (Fig. 5a–c, Supplementary Table 17). Similarly, there were no statistically significant differences in the basal slowing response between *E. coli* OP50- and Δ*bslA B. subtilis*-colonized worms treated with 6-OHDA (Fig. 5a–c, Supplementary Table 17). The *B. subtilis* proficiency in QS was necessary for the complete protection of aged *daf-2*, *clk-1* and *daf-2;clk-1* worms against the effect of 6-OHDA, but the contribution of CSF to this protective effect was less significant than the contribution of *B. subtilis* biofilm. Protection against the effect of 6-OHDA was reduced ~ 25%, ~ 19%, and ~ 22% in Δ*csf B. subtilis*-colonized aged *daf-2*, *clk-1* and *daf-2;clk-1* worms compared with the same worm strains colonized by biofilm-forming *B. subtilis*.

To obtain further insights into the effect of *B. subtilis* against nonaging-related PD, we studied the effect of 6-OHDA treatment on the basal slowing response of *C. elegans* strains in which the expression of signaling molecules related to immunity and the stress response was altered. The dopamine-dependent basal slowing response was unaffected in biofilm-proficient *B. subtilis*-colonized *hsf-1*, *daf-16*, and *daf-16;daf-2* worms after 6-OHDA treatment compared with the responses of 6-OHDA untreated *hsf-1 daf-16* or *daf-16;daf-2* worms colonized by *E. coli* OP50 or biofilm-forming *B. subtilis* (Fig. 5d–f, Supplementary Table 17).

The ability of *B. subtilis* to produce biofilm was crucial for its capability to protect *hsf-1*, *daf-16* and *daf-16;daf-2* worms from the detrimental effects of 6-OHDA compared with similar worms colonized by biofilm-forming *B. subtilis* (Fig. 5d–f, Supplementary Table 17). As observed before, there is not statically significant differences in the basal slowing response between *E. coli* OP50- and Δ*bslA B. subtilis*-colonized aged *hsf-1, daf-16, or daf-16;daf-2* worms treated with 6-OHDA (Fig. 5d–f, Supplementary Table 17). QS proficiency was less crucial (but still significant, $p < 0.001$) than biofilm formation in the ability of *B. subtilis* to protect *hsf-1*, *daf-16* and *daf-16;daf-2 C. elegans* from 6-OHDA-induced dopaminergic neuron injury. Protection against the effect of 6-OHDA was decreased ~ 13%, ~ 22. % and ~ 24% in Δ*csf B. subtilis*-colonized *hsf-1*, *daf-16* and *daf-16;daf-2* worms compared with similar worms colonized by biofilm-forming *B. subtilis*. The overall results suggest that neither aging, HSF-1 nor DAF-16 are related to the protective effect of *B. subtilis* against the damage of dopaminergic neurons induced by treatment with 6-OHDA[35].

The *C. elegans* stress-responsive transcription factor SKN-1 and its mammalian orthologue Nrf-2 (nuclear factor erythroid 2-related factor 2) are under the control of the P38 MAP kinase (PMK-1) signaling pathway[36,37]. Interestingly, SKN-1 and the PMK-1 signaling pathway, which regulates its activity, are required for the protective effect of *B. subtilis* against PD-related dopaminergic neuron injury induced by treatment with 6-OHDA (Fig. 5g,h). The basal slowing response was severely inhibited (~ 60%) in 6-OHDA-treated biofilm-

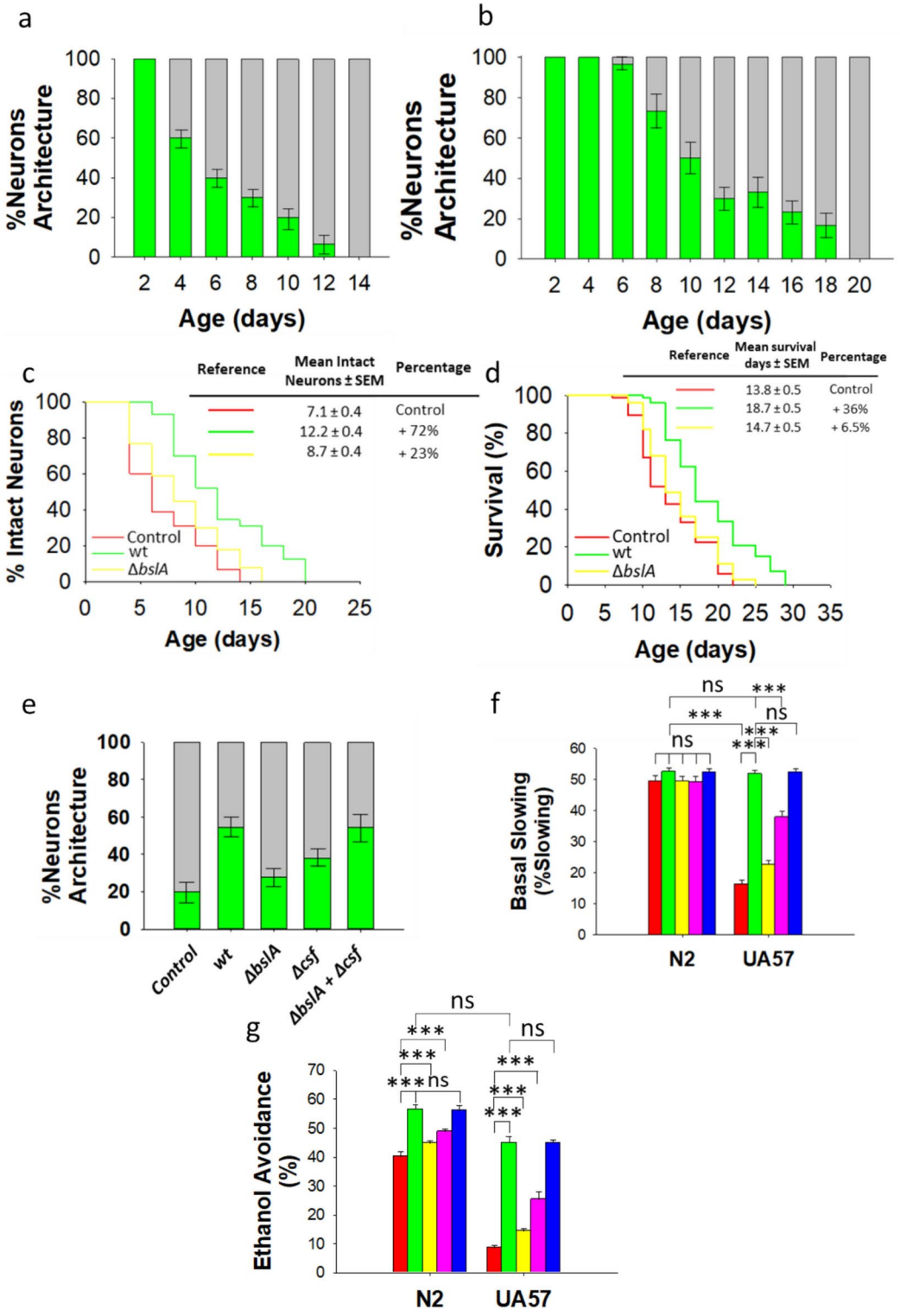

forming *B. subtilis*-colonized *skn-1* or *pmk-1* worms compared with *skn-1* and *pmk-1* worms colonized by *E. coli* OP50 and not treated with 6-OHDA (Fig. 5g,h, Supplementary Table 17). *skn-1* and *pmk-1* worms exhibited the same behavioral change (i.e., impairment of the basal slowing response) in response to treatment with 6-OHDA regardless of whether they were colonized by *E. coli* OP50 or biofilm-forming *B. subtilis*, suggesting that the protective effect of *B. subtilis* against 6-OHDA-induced neuron dopaminergic damage is dependent on SKN-1/PMK-1 signaling. As expected, there were no significant differences in the basal slowing response following 6-OHDA treatment between biofilm-forming and Δ*bslA B. subtilis*-colonized *skn-1* and *pmk-1* worms and *E. coli* OP50-colonized *skn-1* and *pmk-1* worms (Fig. 5g,h, Supplementary Table 17).

◀**Fig. 4**. Biofilm-proficient *B. subtilis* delays early dopaminergic neurodegeneration and improves dopamine-dependent behavior in *C. elegans*. (**a**,**b**) The degeneration of dopaminergic neurons in the head region of UA57 worms colonized by *E. coli* OP50 (**a**) or biofilm-forming *B. subtilis* (**b**). Neuronal degeneration was monitored by semiquantification of the expression of GFP-tagged CEP and ADE dopaminergic neurons. The percentages of worms with normal neuronal integrity (i.e., worms with absence of dopaminergic neuronal damage, green) and worms presenting dopaminergic neuronal damage (gray) are indicated. See the Methods section for details. (**c**,**d**) The percentage of *E. coli* OP50 (red)-, biofilm-forming *B. subtilis* (green)-, or Δ*bslA B. subtilis* (yellow)-colonized UA57 worms exhibiting intact neurons (no loss) over time and the lifespan of these worms (**c**,**d**, respectively). (**e**) Semiquantification of dopaminergic neurodegeneration in 8-day-old UA57 worms colonized by *E. coli* OP50, biofilm-forming *B. subtilis* or its isogenic mutants Δ*bsl*A, Δ*csf*, or equal amounts of Δ*bsl*A and Δ*csf* cells. Semiquantification dopaminergic neurodegeneration data are presented as the average of three biological replicates, and the error bars represent the standard errors of the mean. (**f**,**g**) The basal slowing response (**f**), and the ethanol avoidance (**g**) in 5-day-old N2 and UA57 worms colonized by *E. coli* OP50 (red), biofilm-proficient *B. subtilis* (green), Δ*bsl*A *B. subtilis* (yellow), Δ*csf B. subtilis* (pink), or equal amounts of Δ*bslA* and Δ*csf* cells (blue) are showed. Each graph (**f**,**g**) shows the average ± s.e.m. (n = 3); ns, not significant; $p > 0.05$; *$p < 0.05$; ***$p < 0.001$ (ANOVA followed by Bonferroni's test). Experiments were done by triplicate using 90 animals in each experiment.

Discussion

After Alzheimer's disease, PD is the most common disorder of the human brain for which there are currently no cures, preventive measures, or effective treatments[1,2]. Here, we showed that biofilm-forming *B. subtilis* (Fig. S1) and, to a lesser extent, the QS peptide CSF[26,34] were effective in preventing 6-OHDA-induced damage to dopaminergic neurons and improving dopaminergic-dependent behaviors (Figs. 2 and 5), and in increasing the lifespan (Figs. 3 and 4) of *C. elegans* PD model strains (see Supplementary Table 18 for a resume of the main experimental data presented in this work). Because aging is the main risk factor for the development of PD, it was proposed that strategies that delay aging could be effective in preventing PD[19,20]. As a proof of concept, Cooper et al. showed that delaying aging through interference with ILS signaling was neuroprotective in *C. elegans* models of PD[21]. Importantly, the beneficial effect of delaying aging has been observed in other organisms, such as in *Drosophila* and mice models of PD, and has been suggested in nonhuman primates[20,38–43]. Based on the ability of biofilm-forming *B. subtilis* to delay the aging process of *C. elegans* by decreasing ILS signaling activity[26], we[27] and others[28] demonstrated that probiotic *B. subtilis* strains able to form biofilm (i.e., the DG101[25,27,29–32] and PXN21[28] probiotic strains), and the wild-type (biofilm-forming and non-probiotic) NCIB3610 model strain (Fig. 1), were able to prevent the aggregation of overexpressed GFP-tagged human α-Syn in *C. elegans*. Here, we demonstrated that the protective effects of biofilm-forming *B. subtilis* (Fig. S1) against the PD-related neurotoxin 6-OHDA were not mediated by interference with the ILS signaling (Fig. 5 and Supplementary Table 17), suggesting that there may be other mechanisms (independent of aging) through which biofilm-forming *B. subtilis* protects *C. elegans* from the PD-related 6-OHDA-induced neuron dopaminergic damage.

In addition to aging[19,20,38] and genetic factors[1,2,12], the development of PD is influenced by environmental factors[3,13]. Oxidative stress has been shown to be linked to the initiation and progression of PD[44,45]. Various in vitro and in vivo studies suggest that the development of PD may be initiated by oxidative damage to otherwise healthy neurons caused by etiological factors (e.g., toxins such as MPTP, rotenone, paraquat or 6-OHDA), which activate a cascade of deleterious effects that ultimately injure dopaminergic neurons and lead to PD development[13,35,44,45]. In support of this view, an increased incidence of PD is found in people living in rural areas or urban regions surrounded by farming areas[46]. This is probably because people in rural areas are exposed to pesticides that might cause neuronal oxidative damage in the brain. Specifically, the ability of *B. subtilis* to prevent the 6-OHDA-induced neuron dopaminergic damage described in this work does not involve inhibition of the ILS/DAF-2 (IGFR-1)/DAF-16 (FOXO)-HSF axis, which is downregulated by biofilm-forming *B. subtilis* and associated with aging-related PD[21] (Fig. 5a–f). Our results showed that *daf-2*, *clk-1*, or *daf-2;clk-1* worms colonized by *E. coli* OP50 and treated with 6-OHDA were not protected (Fig. 5a–c). In contrast, *daf-2*, *clk-1*, and *daf-2;clk-1* worms colonized by biofilm-forming *B. subtilis* were protected from the neuron dopaminergic damage caused by 6-OHDA exposure (Fig. 5a–c). Additionally, *hsf-1*, *daf-16*, and *daf-16;daf-2* worms colonized by biofilm-forming *B. subtilis* were protected from the effects of 6-OHDA, while the same type of worms colonized by *E. coli* OP50 were not protected from injury caused by treatment with 6-OHDA (Fig. 5d–f). We demonstrate that the effect of biofilm-forming *B. subtilis* against 6-OHDA treatment requires the activity of the PMK-1/SKN-1 signaling axis in *C. elegans* (Fig. 5g,h). *C. elegans* manages stress through the activation and inhibition of the PMK-1 (p38MAPK in mammals) and ILS—DAF-2 (ILS—IGFR-1 in mammals) signaling pathways, respectively[48–50]. The activation of PMK-1 signaling and/or the inhibition of ILS signaling allows the nuclear translocation of active SKN-1 and DAF-16, respectively[50]. DAF-16 and SKN-1 (FOXO and Nrf2 in mammals, respectively) are major regulators of genes involved in detoxification and antioxidant defense[47–49]. The findings presented here linking the effect of biofilm-forming *B. subtilis* against neuron dopaminergic injury to SKN-1 in *C. elegans* are consistent with three phenomena observed in humans with PD: (1) loss of function mutations in *PARK-7* (also known as *DJ-1*), which product PARK-7 stabilizes Nrf2, leads to early onset of human PD[8,50]; (2) Nrf2 activation ameliorates neurodegeneration in clinical and preclinical models of PD[51–53]; and (3) the gut microbiome of PD patients is depleted of sporulation genes (e.g., *B. subtilis* genes)[54], and this deficiency in sporulation genes is linked to constipation[32], which is the earliest sign of PD[14,15] and can precede motor signs by decades[14,32,54].

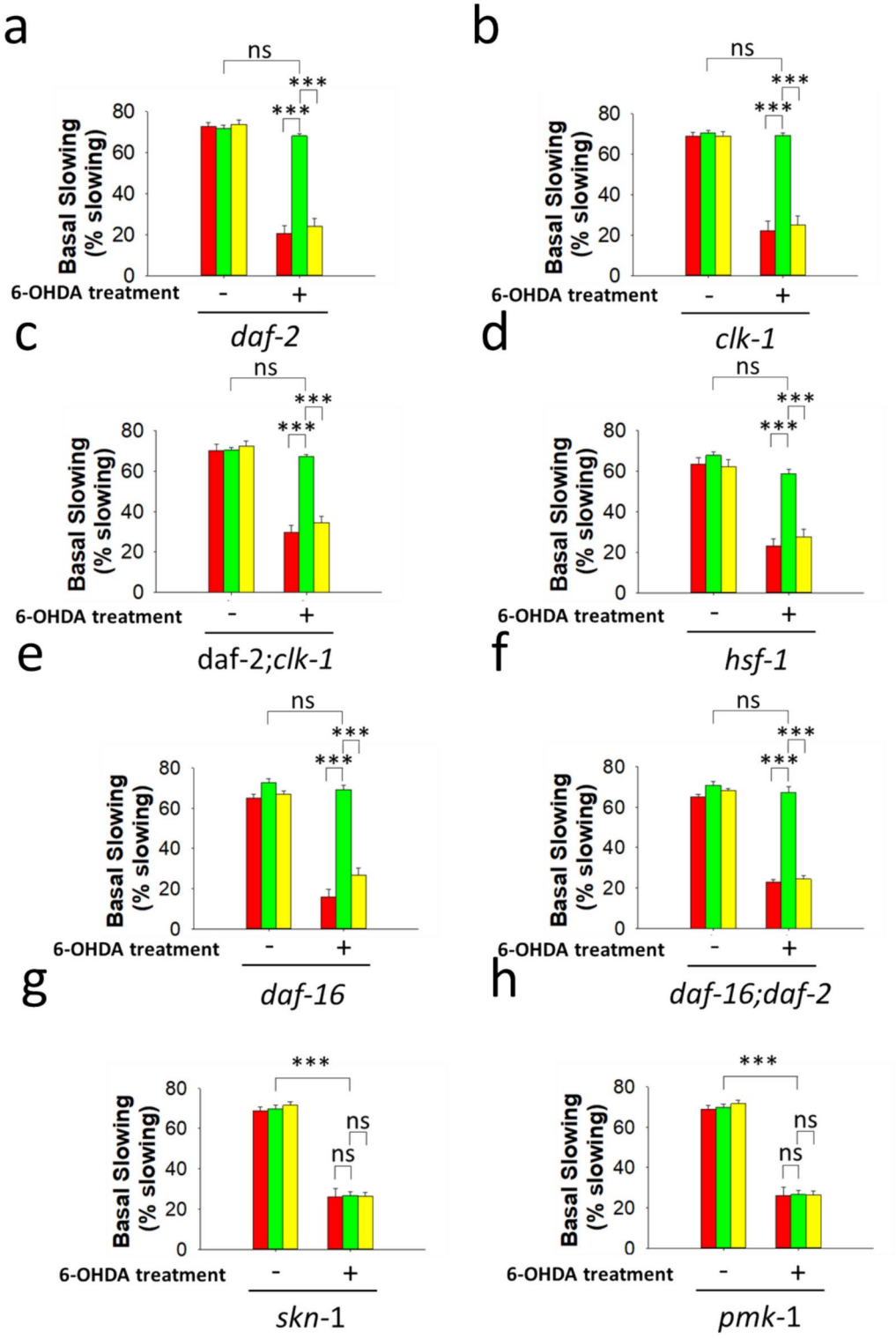

Fig. 5. Biofilm-proficient *B. subtilis* protects *C. elegans* from PD-associated dopaminergic 6-OHDA damage through PMK-1/p38 MAPK and SKN-1/Nrf2 signaling. (**a**) Basal slowing responses in 8-day-old adult *daf-2* (**a**), *clk-1* (**b**), *daf-2;clk-1* (**c**), *hsf-1* (**d**), *daf-16* (**e**), *daf-16;daf-2* (**f**), *skn-1* (**g**), and *pmk-1* (**h**) worms treated with or without 75 mM 6-OHDA as indicated in "Methods" section. Worms (**a**–**h**) were colonized by *E. coli* OP50 (red), biofilm-proficient *B. subtilis* (green), or Δ*bslA B. subtilis* (yellow). Each graph (**a**–**h**) shows the average ± s.e.m. (n = 3); *ns* no significant difference; $p > 0.05$; $^{***}p < 0.001$ (ANOVA followed by Bonferroni's test). Experiments were done by triplicate using 90 animals in each experiment.

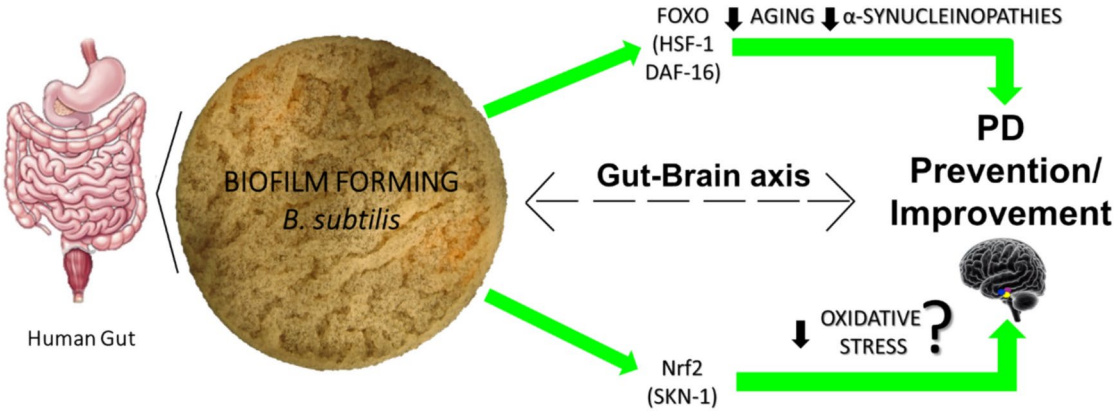

Fig. 6. Working model of the possible protective effect of biofilm-forming *B. subtilis* against PD. The cartoon summarizes how biofilm-forming *B. subtilis* in the human gut could protect against PD via the simultaneous regulation (inhibition and activation) of two independent signaling pathways linked to aging progression, alpha-synucleinopathies protection (the ILS-IGFR-1/FOXO pathway), and the oxidative stress response (the p38MAPK/Nrf2 pathway), respectively, that impact on PD susceptibility. The colored ovals in the brain denote the three area of dopaminergic neurons that might be protected by gut *B. subtilis* in the human midbrain ("gut-brain axis"). Violet oval: retrorubral field (RRF, A8, mesolimbic pathway); yellow oval: substantia nigra pars compacta (SNc, A9, nigrostriatal pathway); and blue oval: ventral tegmental area (VTA, A10, mesocortical pathway). MF is the author of this figure, see text for details.

Because multiple factors underlie the pathology and progression of PD, it is plausible that single-target-based therapeutic strategies will be not clinically beneficial[1,2]. Therefore, it has been hypothesized that treatment approaches for PD should involve a cocktail of different agents or therapies, each targeting different key factors (in this sense, *B. subtilis* simultaneously could shields against alpha-synuclein β-sheet aggregation, aging progression and dopaminergic neuron injury) that predispose people to the development and progression of PD[18,32,55,56]. The present work opens the tempting possibility that biofilm-forming *B. subtilis* might help to ameliorate PD and other dopamine-related neuropathies[55–58] (Fig. 6).

Methods

Strains and growth media

The *B. subtilis* strains used in this study were the wild-type and biofilm-proficient NCIB3610 model strain and, its isogenic derivatives RG3603 (NCIB3610 Δ*bslA*::phe^r) and RG4010 (NCIB3610 Δ*csf*::tet^r)[26]. The *E. coli* strain OP50 was obtained from the *Caenorhabditis* Genetic Center (CGC). Bacteria were grown in Luria–Bertani (LB) broth and Schaeffer's sporulation medium (SM) at 37 °C for 24 and 48 h, respectively. Bacterial cultures were diluted 1/100 for seeding. Sporulation was induced by the starvation method[26]. Briefly, *B. subtilis* strains were grown in SM at 37 °C for 48 h. After this incubation period, the cultures were heat-treated for 20 min at 80 °C to kill vegetative cells[26]. To obtain pure spores, the heat-treated cultures were treated three times with lysozyme (25 mg ml^{-1}; Sigma Co.), washed with cold water after each lysozyme treatment and centrifuged until 100% of the culture consisted of phase-bright spores.

The following *C. elegans* strains used in this study were obtained from CGC: N2 (wild-type Bristol strain), BZ555 egIs1 [*dat-1p*::GFP], CB1370 *daf-2*(e1370) III, CF1038 *daf-16*(mu86) I, EU1 *skn-1*(zu67) IV, HT1890 *daf-16*(mgDf50) I—*daf-2*(e1370) III, KU25 *pmk-1*(km25) IV, MQ130 *clk-1*(qm30) III, MQ513 *daf-2*(e1370) *clk-1*(e2519) III, NL5901 pkIs2386[*punc-54*:: *α-synuclein*::YFP + *unc-119*(+)], PS3551 *hsf-1*(sy441) I, UA57 baIs4 [*dat-1*p::GFP + *dat-1*p::CAT-2], and VC1024 *pdr-1*(gk448) III. These worm strains were maintained on Nematode Growth Medium agar (NGM) plates seeded with OP50 *E. coli* cells at 20 °C, except for strains harboring the *daf-2* mutation, which were maintained at 16 °C to avoid dauer formation. Late L4/young adult stage worms were washed three times to remove residual *E. coli* OP50, placed on NGM plates with a lawn of the *B. subtilis* strain of interest and incubated at 20 °C for phenotyping assays[26].

6-Hydroxydopamine treatment

6-Hydroxydopamine (6-OHDA) was obtained from Sigma Aldrich. In brief, L1 larvae were raised on NGM agar plates seeded with a lawn of *E. coli* OP50 until the L3 stage. Then, the L3 larvae were washed three times with distilled water to remove residual bacteria, transferred to a 1.5 mL Eppendorf tube containing 100 µL of different concentrations of 6-OHDA and 10 mM ascorbic acid, and incubated for 1 h at 20 °C with gentle mixing every 10 min. After 1 h of treatment, the L3 larvae were washed three times with M9 buffer (22 mM KH_2PO_4, 34 mM K_2HPO_4, 86 mM NaCl, and 1 mM $MgSO_4$) and then raised on NGM plates seeded with the corresponding bacteria until they reached the adult stage[3,50]. For the control experiments, L3 larvae were washed and processed in the same way as mentioned for the 6-OHDA-treated L3 larvae, with the exception that 6-OHDA was omitted.

Lifespan analysis

Lifespan was assessed at 20 °C as described previously[26]. A synchronous population was obtained by treating gravid hermaphrodites with sodium hypochlorite to obtain eggs, which were subsequently raised on standard NGM plates. Late L4/young adult stage worms were used at t = 0 for lifespan analysis and then transferred to fresh plates every 2 days. During the quantification of the number of dead/live worms, the operator was blinded to the groups. All the experiments were repeated at least three times. Worms were considered dead when pharyngeal pumping ceased and they did not respond to prodding with a platinum wire. Worms with internal hatching were removed from the plates and excluded from lifespan calculations.

Locomotion

Locomotion was assessed by measuring thrashing in liquid medium[26]. In brief, on day 5 of adulthood, worms were washed three times in M9 buffer to remove residual bacteria. The cleaned worms were placed in M9 buffer on a clean NGM plate. Trashing was quantified by counting the number of body bends over 20 s for each worm under a stereomicroscope (Zeiss Stemi 305).

Basal slowing response

The basal slowing response was evaluated as described previously[21]. Assay plates were prepared by spreading bacteria, i.e., *E. coli* (OP50), on NGM agar, and together with unseeded assay plates, the seeded assay plates were incubated at 37 °C overnight and cooled to room temperature prior to the assay. On day 5 of adulthood, worms were washed three times with M9 buffer, placed on NGM plates without bacteria and incubated for 1 h at 20 °C. Afterward, the worms were transferred to the bacteria-containing or unseeded assay plates described above and allowed to settle for 5 min, after which the number of body bends in 20 s intervals was recorded. The basal slowing response was calculated as the rate of movement on bacteria-containing plates divided by the rate of movement on unseeded plates.

Dopaminergic neurodegeneration

Neurodegeneration of dopaminergic neurons was analyzed as described previously[21]. BZ555 and UA57 worms were washed three times with M9 buffer, mounted onto a 2% agar pad on a glass slide, immobilized using 0.25 mM sodium azide (NaN_3, Sigma Co.), and covered with a coverslip. Dopamine neuron morphology in the head region [four cephalic (CEP) and two anterior deirid (ADE) neurons] in worms of different ages was evaluated by observing the expression of GFP under the control of the *dat-1* promoter in dopamine neurons using an Olympus FV1000 laser confocal scanning microscope. The finding that all six dopaminergic neurons were intact, was scored as "absence of dopaminergic neuronal damage". The finding of at least one sign of neuronal deterioration (for example, loss of some or parts of neurons, loss of neuronal cell bodies, the absence of neuronal processes, breakage of neurites, shrinking of dendritic endings, or the presence of neuritic blebbing) was scored as "presence of dopaminergic neuronal damage". The images were analyzed with Olympus software and Fiji software.

Fecundity

Fecundity was measured via a progeny count assay[26]. In brief, L4 worms were individually placed onto NGM plates seeded with different bacteria. The worms were transferred every day to fresh plates until the end of their reproductive phase or death. The eggs laid by the adults each day were allowed to develop for 48 h at 20 °C and then manually counted to determine the number of progeny produced by each individual on each day. Fecundity was calculated ass the sum of all the progeny worms obtained throughout the reproductive stage. Worms that died during the reproductive stage were excluded.

Ethanol avoidance response

An ethanol avoidance assay was performed as described previously[26]. In brief, 10 cm diameter Petri dishes containing 25 ml of 2% agar, 5 mM KPO_4 [pH 6], 1 mM $CaCl_2$, and 1 mM $MgSO_4$ were used assay plates. On the back of the assay plates, a 2.5 cm diameter circle was drawn in the center of the plate. From that central circle, the plates were divided into 4 quadrants (2 test quadrants facing each other and 2 control quadrants facing each other). In addition, approximately 0.5 cm from the edge of the agar in each quadrant, a mark was made. Two microliters of absolute ethanol were placed on the agar on top of the mark in the test quadrants, and 2 µl of distilled water was placed on the agar on top of the mark in the control quadrants. Additionally, 1 µl of 1 M NaN_3 was applied on top of each mark to immobilize the worms when they entered a new quadrant. On day 5 of adulthood, worms were washed three times in M9 buffer and one time with distilled water and placed on the center circle on the assay plate. After 1 h of incubation at 20 °C, ethanol avoidance was calculated as {[number of entries into the test quadrants] − [number of entries into the control quadrants]}.

Heat stress

Thermotolerance assays were performed as previously described[26]. Briefly, worms were raised on NGM agar plates at 20 °C until they reached the late L4/young adult stage, and then the adult worms were transferred to fresh NGM plates seeded with the indicated bacteria every 24 h. NGM plates containing *E. coli*- or *B. subtilis*-colonized worms were transferred to 35 °C when the worms reached the age of 5 days. Individuals plates were removed (in triplicate) from the high-temperature environment every hour, and the worms were scored for signs of life as described in the "Lifespan analysis" section above.

Measurement of human α-synuclein aggregation

Seven-day-old NL5901 worms were washed three times with M9 buffer, mounted onto a 2% agar pad on a glass slide, immobilized using 025 mM NaN_3 (Sigma Co.), and covered with a coverslip. Images of the immobilized animals were obtained using an Olympus FV1000 laser confocal scanning microscope. Aggregates were defined as clusters of at least 4 pixels whose intensity was at least 1 standard deviation above the background intensity. Images were analyzed with Olympus software and Fiji software[27,28].

Statistical analysis

All assays were performed at least in triplicate and analyzed with Sigmaplot software, version 14.0, unless otherwise indicated. For survival analysis (Oasis survival software, https://sbi.postech.ac.kr/oasis/), the mean survival duration in days, standard errors, 95% confidence intervals and *P* values were calculated by the log-rank and Kaplan–Meier tests using OASIS software. For data related to neurodegeneration, statistical significance was calculated using the chi-square test with Yates' correction in Microsoft Excel software. For the remaining data, the statistical significance of differences between group was evaluated using ANOVA followed by Bonferroni's test. $^{*}p < 0.05$; $^{**}p < 0.01$; $^{***}p < 0.001$; ns $p > 0.05$.

Data availability

All data generated or analysed during this study are included in this published article (and its supplementary information files). It can also contact the corresponding author for additional requests.

Received: 5 June 2024; Accepted: 10 March 2025
Published online: 21 March 2025

References

1. Obeso, J. A. et al. Past, present, and future of Parkinson's disease: a special assay on the 200th anniversary of the shaking palsy. *Mov. Disord.* **32**, 1264–1310 (2017).
2. Dorsey, E., Sherer, T., Okun, M. & Bloem, B. The emerging evidence of the Parkinson pandemic. *J. Park. Dis.* **8**, S3–S8. https://doi.org/10.3233/JPD-1814474 (2018).
3. Giguére, N., Nanni, S. B. & Trudeau, L. E. On cell loss and selective vulnerability of neuronal populations in Parkinson's disease. *Front. Neurol.* **9**, 455. https://doi.org/10.3389/fneur.2018.00455 (2018).
4. Polymeropoulos, M. H. et al. Mutation in the α-synuclein gene identified in families with Parkinson's disease. *Science* **276**, 2045–2047. https://doi.org/10.1126/science.276.5321.2045 (1997).
5. Bendor, J., Logan, T. & Edwards, R. The function of α-Synuclein. *Neuron.* **79**, 6. https://doi.org/10.1016/j.neuron.2013.09.004 (2013).
6. Hallacli, E. et al. The Parkinson's disease protein alpha-synuclein is a modulator of processing bodies and mRNA stability. *Cell* **185**, 2035–2056. https://doi.org/10.1016/j.cell.2022.05.008 (2022).
7. Alafuzoff, I. & Hartikainen, P. Alpha-synucleinopathies. *Hanbd. Clin. Neurol.* **145**, 339–353 (2017).
8. Bonifati, V. et al. Mutations in the DJ-1 gene associated with autosomal recessive early-onset parkinsonism. *Science* **299**, 256–259. https://doi.org/10.1126/science.1077209 (2003).
9. Lücking, C. B. et al. Association between early-onset Parkinson's disease and mutations in the Parkin gene. *N. Engl. J. Med.* **342**, 1560–1567. https://doi.org/10.1056/nejm200005253422103 (2000).
10. Valente, E. M. et al. Hereditary early-onset Parkinson's disease caused by mutations in PINK1. *Science* **304**, 1158–1160. https://doi.org/10.1126/science.1096284 (2004).
11. Zimprich, A. et al. Mutations in LRRK2 cause autosomal-dominant parkinsonism with pleomorphich pathology. *Neuron* **44**, 601–607 (2004).
12. Klein, C. & Westerberger, A. Genetics of Parkinson's disease. *Cold Spring Harb. Perspect. Med.* **2**, a008888 (2012).
13. Chen, Y. et al. Non-genetic risk factors for Parkinson's disease: an overview of 46 systematic reviews. *J. Park. Dis.* **11**, 919–935. https://doi.org/10.3233/JPD-202521 (2021).
14. Cersosimo, M. G. et al. Gastrointestinal manifestations in Parkinson's disease: prevalence and occurrence before motor symptoms. *J. Neurol.* **260**, 1332–1338. https://doi.org/10.1007/s00415-012-6801-2 (2013).
15. Pfeiffer, R. F. Gastrointestinal dysfunction in Parkinson's disease. *Curr. Treat. Opt. Neurol.* **20**, 54. https://doi.org/10.1007/s11940-018-0539-9 (2018).
16. Liddle, R. A. Parkinson's disease from the gut. *Brain Res.* **1693**, 201–206. https://doi.org/10.1016/j.brainres.2018.01.010 (2018).
17. Gold, A., Turkalp, Z. T. & Munoz, D. G. Enteric alpha-synuclein expression is increased in Parkinson's disease but not Alzheimer's disease. *J. Mov. Disord. Soc.* **28**, 237–240. https://doi.org/10.1002/mds.25298 (2013).
18. Franco, R., Rivas-Santisteban, R., Reyes-Resina, I., Navarro, G. & Martínez-Pinilla, E. Microbiota and other preventive strategies and non-genetic risk factors in Parkinson's disease. *Front. Aging Neurosci.* **12**, 12. https://doi.org/10.3389/fnagi.2020.00012 (2020).
19. Levy, G. The relationship of Parkinson disease with aging. *Arch. Neurol.* **64**, 1242–1246 (2007).
20. Rodriguez, M., Rodriguez-Sabate, C., Morales, I., Sanchez, A. & Sabate, M. Parkinson's disease as a result of aging. *Aging Cell* **14**, 293–308 (2015).
21. Cooper, J. et al. Delaying aging is neuroprotective in Parkinson's disease: a genetic analysis in *C. elegans* models. *Nat. Parkin. Dis.* **1**, 15022. https://doi.org/10.1038/npjparkd.2015.22 (2015).
22. Suh, Y. et al. Functionally significant insulin-like growth factor I receptor mutations in centenarians. *Proc. Natl. Acad. Sci. USA* **105**, 3438–3442 (2008).
23. Ilinskaya, O. N., Ulyanova, V. V., Yarullina, D. R. & Gataullin, I. G. Secretome of intestinal *Bacilli:* a natural guard against pathologies. *Front. Microbiol.* **8**, 1666. https://doi.org/10.3389/fmicb.2017.01666 (2017).
24. Piewngam, P. et al. Pathogen elimination by probiotic *Bacillus* via signalling interference. *Nature* **562**, 532–537. https://doi.org/10.1038/s41586-018-0616-y (2018).
25. Leñini, C. et al. Probiotic properties of *Bacillus subtilis* DG101 isolated from the traditional Japanese fermented food natto. *Front. Microbiol.* **14**, 1253480. https://doi.org/10.3389/fmicb.2023.1253480 (2023).
26. Donato, V. et al. *Bacillus subtilis* biofilm extends *Caenorhabditis elegans* longevity through downregulation of the insulin-like signalling pathway. *Nat. Commun.* **8**, 1–15. https://doi.org/10.1038/ncomms14332 (2017).
27. Grau, R. & Francisco, M. Probiotic *Bacillus subtilis* DG101 prevents alpha-synuclein aggregation and extends the healthy lifespan in Parkinson disease model *Caenorhabditis elegans*. Advances in Alzheimer & Parkinson Therapies AN AAT/AD Focus Meeting; Torino, Italy. https://www.alzforum.org/news/conference-coverage/do-immune-responses-promote-or-prevent-parkinsons-disease (2018).

28. Goya, M. E. et al. Probiotic *Bacillus subtilis* protects against α-synuclein aggregation in *C. elegans*. *Cell Rep.* **30**, 367–3807. https://doi.org/10.1016/j.celrep.2019.12.078 (2020).
29. Rodriguez, A. F., Cardinali, N. & Grau, R. Efficient weight loss and type II diabetes control in overweight and obese patients consuming the probiotic *Bacillus subtilis* DG101: a randomized double-blind placebo-controlled study. *Asploro J. Biomed. Clin. Case Rep.* **5**(1), 51–58. https://doi.org/10.36502/2022/ASJBCCR.6263 (2022).
30. Cardinali, N., Rodriguez, A. F., Leñini, C. & Grau, R. Efficacy of the probiotic *Bacillus subtilis* DG101 to prevent overweight in healthy individuals: a double blind, placebo-controlled study. *J. Obes. Fit. Manag.* https://doi.org/10.58489/2836-5070/013 (2024).
31. Rodriguez, A. F., Leñini, C., Cardinali, N. & Grau, R. A double blind, placebo-controlled study to evaluate the efficacy of probiotic *Bacillus subtilis* DG101 in maintaining blood sugar homeostasis in healthy adults. *Ann. Clin. Med. Case Rep. Rev.* https://doi.org/10.47991/2834-5231/ACMCRR-118 (2024).
32. Cardinali, N., Rodriguez, A. F., Leñini, C., Perez, O. & Grau, R. Efficacy of the probiotic *Bacillus subtilis* DG101 against intestinal disconfort and constipation in healthy adults: a double-blind, placebo-controlled study. *Am. J. Clin. Med. Res.* https://doi.org/10.47991/2835-9496/AJCMR-129 (2024).
33. Smolentseva, O. et al. Mechanism of biofilm-mediated stress resistance and lifespan extension in *C. elegans*. *Sci. Rep.* **7**, 7137. https://doi.org/10.1038/s41598-017-07222-8 (2017).
34. Fujiya, M. et al. The *Bacillus subtilis* quorum-sensing molecule CSF contributes to intestinal homeostasis via OCTN2, a host cell membrane transporter. *Cell Host Microbe* **1**, 299–308 (2007).
35. Cao, S., Gelwix, C. C., Caldwell, K. A. & Caldwell, G. A. Torsin-mediated protection from cellular stress in the dopaminergic neurons of *Caenorhabditis elegans*. *J. Neurosci.* **25**, 3801–3812. https://doi.org/10.1523/JNEUROSCI.5157-04.2005 (2005).
36. Troemel, E., Chu, S., Reinke, V., Ausubel, F. & Kim, D. p38 MAPK regulates expression of immune response genes and contributes to longevity in *C. elegans*. *PLoS Genet.* **2**, e183. https://doi.org/10.1371/journal.pgen.0020183 (2006).
37. Hu, Q., D'Amora, D., MacNeil, L., Walhout, A. & Kubiseski, T. The oxidative stress response in *Caenorhabditis elegans* requires the GATA transcription factor ELT-3 and SKN-1/Nrf2. *Genetics.* **206**, 1909–1922. https://doi.org/10.1534/genetics.116.198788 (2017).
38. Collier, T. J., Kanaam, N. M. & Kordower, J. H. Ageing as a primary risk factor for Parkinson's disease: evidence from studies of non-human primates. *Nat. Rev. Neurosci.* **12**, 359–366 (2011).
39. Harrison, D. E. et al. Rapamycin fed late in life extends lifespan in genetically heterogeneous mice. *Nature* **460**, 392–395 (2009).
40. Maswood, N. et al. Caloric restriction increases neurotrophic factor levels and attenuates neurochemical and behavioral deficits in a primate model of Parkinson's disease. *Proc. Natl. Acad. Sci. USA* **101**, 18171–18176 (2004).
41. Onken, B. & Driscoll, M. Metformin induces a dietary restriction-like state and the oxidative stress response to extend *C. elegans* Healthspan via AMPK, LKB1, and SKN-1. *PLoS One* **5**, e8758 (2010).
42. Patil, S. P., Jain, P. D., Ghumatkar, P. J., Tambe, R. & Sathaye, S. Neuroprotective effect of metformin in MPTP-induced Parkinson's disease in mice. *Neuroscience* **277**, 747–754 (2014).
43. Bluher, M., Kahn, B. B. & Kahn, C. R. Extended longevity in mice lacking the insulin receptor in adipose tissue. *Science* **299**, 572–574 (2003).
44. Henchcliffe, C. & Beal, M. F. Mitochondrial biology and oxidative stress in Parkinson's disease pathogenesis. *Nat. Clin. Pract. Beurol.* **4**, 600–609 (2008).
45. Zhou, C., Huang, Y. & Przedborski, S. Oxidative stress in Parkinson's disease, a mechanism of pathologic and therapeutic significance. *Ann. N. Y. Acad. Sci.* **1147**, 93–104. https://doi.org/10.1196/annals.1427.023 (2008).
46. Gorrel, J. M., Johnson, C. C., Rybicki, B. A., Peterson, E. L. & Richardson, R. J. The risk of Parkinson's disease with exposure to pesticides, farming, well water, and rural living. *Neurology* **50**, 1346–1350. https://doi.org/10.1212/wnl:1346-50 (1998).
47. Vanduyn, N., Settivari, R., Wong, G. & Nass, R. SKN-1/Nrf2 inhibits dopamine neuron degeneration in a *Caenorhabditis elegans* model of methylmercury toxicity. *Toxicol. Sci.* **118**, 613–624. https://doi.org/10.1093/toxsci/kfq285 (2010).
48. Settivari, R., VanDuyn, N., LeVora, J. & Nass, R. The Nrf2/SKN-1-dependent glutathione S-transferase π homologue GST-1 inhibits dopamine neuron degeneration in a *Caenorhabditis elegans* model of manganism. *Neuro Toxicol.* **38**, 51–60. https://doi.org/10.1016/j.neuro.2013.05.014 (2013).
49. Keshet, A. et al. PMK-1 p38 MAPK promotes cadmium stress resistance, the expression of SKN-1/Nrf and DAF-16 target genes, and protein biosynthesis in *Caenorhabditis elegans*. *Mol. Genet. Genom.* **292**, 1341–1361. https://doi.org/10.1007/s00438-017-1351-z (2017).
50. Clements, C., McNally, R., Conti, B., Mak, T. & Ting, J. DJ-1, a cancer- and Parkinson's disease-associated protein, stabilizes the antioxidant transcriptional master regulator Nrf2. *Proc. Natl. Acad. Sci.* **103**, 15091–15096. https://doi.org/10.1073/pnas.0607260103 (2006).
51. Parga, J. A., Rodriguez-Perez, A. I., Garcia-Garrote, M., Rodriguez-Pallares, J. & Labandeira-García, J. Nrf2 activation and downstream effects: focus on Parkinson's disease and brain angiotensin. *Antioxidans* **10**, 1649. https://doi.org/10.3390/antiox10111649 (2021).
52. Yang, X.-X., Yang, R. & Zhang, F. Role of Nrf2 in Parkinson's disease: toward new perspectives. *Front. Pharmacol.* **13**, 919233. https://doi.org/10.3390/fphar.2022.919233 (2022).
53. Segura-Aguilar, J. & Mannervik, B. A preclinical model for Parkinson's disease based on transcriptional gene activation via KEAP1/NRF2 to develop new antioxidant therapies. *Antioxidants* **12**, 673. https://doi.org/10.3390/antiox12030673 (2023).
54. Wallen, Z. et al. Metagenomics of Parkinson's disease implicates the gut microbiome in multiple disease mechanisms. *Nat. Commun.* **13**, 6958. https://doi.org/10.1038/s41467-022-34667-x (2022).
55. Larroya-García, A., Navas-Carrillo, D. & Orenes-Piñero, E. Impact of gut microbiota on neurological diseases: Diet composition and novel treatments. *Crit. Rev. Food Sci. Nutr.* **59**, 3102–3116. https://doi.org/10.1080/10408398.2018.1484340 (2019).
56. Van Bulck, M., Sierra-Magro, A., Alarcon-Gil, J., Perez-Castillo, A. & Morales-Garcia, J. A. Novel approaches for the treatment of Alzheimer's and Parkinson's disease. *Int. J. Mol. Sci.* **20**, 719. https://doi.org/10.3390/ijms20030719 (2019).
57. Ayala, F. R. et al. Microbial flora, probiotics, *Bacillus subtilis* and the search for a long and healthy human longevity. *Microb. Cell.* **16**(4), 133–136. https://doi.org/10.15698/mic2017.04.569 (2017).
58. Roeper, J. Dissecting the diversity of midbrain dopamine neurons. *Trends Neurosci.* **36**, 336–342. https://doi.org/10.1016/j.tins.2013.03.003 (2013).

Acknowledgements

We thank technical staff of the laboratory for their technical assistance in the described experiments. We also thank all current and former laboratory members, especially Cira Crespo and Juan Alberto Guarrochena, for their technical assistance and thoughtful discussions, respectively.

Author contributions

All authors (M.G.F. and R.G.) made substantial contributions to the conception and design of the study and analysis and interpretation of the results. R.G. revised and wrote the manuscript. All authors approved the final version of the manuscript.

Competing interests
The authors declare no competing interests.

Additional information
Supplementary Information The online version contains supplementary material available at https://doi.org/10.1038/s41598-025-93737-4.

Correspondence and requests for materials should be addressed to R.G.

Reprints and permissions information is available at www.nature.com/reprints.

Publisher's note Springer Nature remains neutral with regard to jurisdictional claims in published maps and institutional affiliations.